Available online at www.sciencedirect.com
ScienceDirect
Mathematics and Computers in Simulation 81 (2010) 76–91
MATHEMATICS AND COMPUTERS IN SIMULATION
www.elsevier.com/locate/matcom

A finite element approach for multiphase fluid flow in porous media

Javier L. Mroginski [a,c,*], H.Ariel Di Rado [a], Pablo A. Beneyto [a], Armando M. Awruch [b]

[a] *Departamento de Mecánica Aplicada. Facultad de Ingeniería, Universidad Nacional del Nordeste (UNNE), Av. Las Heras 727, Resistencia (CP:3500), Argentina*

[b] *Centro de Mecánica Aplicada y Computacional (CEMACOM), Universidad Federal do Rio Grande do Sul (UFRGS), Brazil*

[c] *CONICET, Consejo Nacional de Investigaciones Científicas y Técnicas, Argentina*

Received 28 September 2009; received in revised form 22 March 2010; accepted 1 July 2010
Available online 13 July 2010

Abstract

The main scope of this work is to carry out a mathematical framework and its corresponding finite element (FE) discretization for the partially saturated soil consolidation modelling in presence of an immiscible pollutant. A multiphase system with the interstitial voids in the grain matrix filled with water (liquid phase), water vapour and dry air (gas phase) and with pollutant substances, is assumed. The mathematical model addressed in this work was developed in the framework of mixture theory considering the pollutant saturation–suction coupling effects. The ensuing mathematical model involves equations of momentum balance, energy balance and mass balance of the whole multiphase system. Encouraging outcomes were achieved in several different examples.

Keywords: Consolidation; Immiscible pollutants; Finite elements; Multiphase porous media; Mixture theory

1. Introduction

Environmental geomechanics spans a wide number of engineering problems where the geomaterials mechanical equations are usually coupled with flux and mass transport equations. This area generally deals with pollutant transport problems through aquifers, especially when partially saturated media is involved, because, under these circumstances, the solid phase usually undergoes large deformation and displacement due to the proper soil nature or due to the capillary pressure effect. Another relevant aspect of the environmental geomechanics science is to design safe containers free of toxic and/or nuclear wastes or pollutant leftovers [1]. For this reason, it is a matter of prior importance in industrial societies.

Different authors have taken over this issue from several standpoints regarding different aspects or hypothesis. An early view of the problem may be found in Li and Zienkiewicz [16]. In this work, the fluid transport through porous media is simultaneously presented in one or two phases separated by an interface. No chemical reactions or components interchange between the phases are regarded and the capillary pressure is given in series form. In Schrefler [20], a mathematical framework assuming a multiphase porous system with voids filled with water, water vapour, dry air and pollutant along with a finite element (FE) discretization according to the mixture theory, is presented. Here, the

* Tel.: +54 3722 420076; fax: +54 3722 420076.
E-mail address: javierm@ing.unne.edu.ar (J.L. Mroginski).
URL: http://ing.unne.edu.ar/mecap/ (J.L. Mroginski).

0378-4754/$36.00 © 2010 IMACS. Published by Elsevier B.V. All rights reserved.
doi:10.1016/j.matcom.2010.07.001

pollutants may be mixed with the fluid phase or they may not, in which case, a new phase wherein this pollutants flow (immiscible phase) is considered. Similarly to the previous work, no chemical reaction between pollutant and the other phases is allowed.

Sheng and Smith [23] presented a two-dimensional FE solution for various contaminants considering advection–dispersion transport, which is based on a previous work [22]. Juncosa et al. [10] assert the basic postulated for a mathematical framework for non-isothermal multiphase flux with reactive transport and the solution for this problem is undertaken. The media constituent mass balance (water, air and solute), the energy conservation principle and the equilibrium equations, describe a partial derivative system of equations that may be integrated using various approaches. In Klubertanz et al. [12], the mathematical framework for the analysis of the miscible and immiscible flux through porous media, based on continuum mechanics, was presented.

Finally, in Schrefler [20] and later on in Schrefler and Pesavento [21], relying on Hassanizadeh and Gray averaging theories [7–9], the analysis of isothermal flux transport was further extended to non-isothermal flux, bearing in mind the thermodynamics properties of the interface between the different porous media constituents [15]. In fact, the interface surface tension holds the immiscibility between porous fluids. A null value of the surface tension implies in a null value of the capillary pressure as well, bringing on a constant fluid pressure.

In the present work, the analysis of immiscible pollutant transport through partially saturated soils, coupled with the mechanical behaviour, is undertaken. A mathematical framework assuming a multiphase porous media, where the interstitial voids of the solid matrix are filled with water, dry air and pollutant, is addressed and the solution of the partial difference equation system is solved using the FE method. The numerical model involves momentum, energy and mass balance equations. Some numerical examples are also included in order to validate the model.

2. Representative elemental volume

In classical mechanics, a continuum distribution of particles (fluids or solids), for which the balance laws and constitutive relationships are valid, is taken for granted. The phenomena to be studied here, occurs in domains occupied by different phases. There is an omnipresent phase, i.e., the solid skeleton, whose voids are taken to be filled with fluid (gas or liquid) separated by a membrane called interface. The difference between constituents and phases should be emphasised here: the phases are chemically homogeneous portions of the multiphase system, which mechanical behaviour is assumed to be uniform. On the other hand, the constituents are the individual parts that yield the phases but acting each one independently; the gaseous phase may be constituted by a gas mix, with several constituents.

There are two possible levels to describe the multiphase media intergranular configuration: the macroscopic and the microscopic level. At the microscopic level, the real porous media structure is regarded (see Fig. 1). The governing equations are established considering each constituent separately, giving rise to a complicated solution. Furthermore, the microscopic properties are usually awkward to assess. Considering the aforementioned reasons and adding that a microscopic description is far beyond the civil engineering goals, for the present work, a macroscopic description is adopted. One noteworthy feature of the macroscopic description is the fact that at each material point all the phases are assumed to be simultaneously present. In a volume fraction, the following elements may be found:

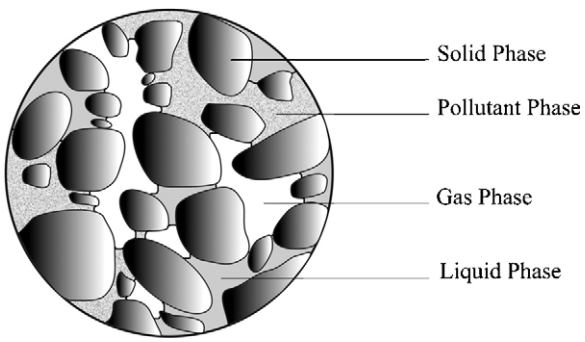

Fig. 1. Multiphase medium: representative elemental volume at microscopic level.

- Solid phase: $\eta^s = 1 - n$, being $n = (dv^w + dv^g + dv^\pi)/dv$ the porosity and dv^i the differential volume of the i constituent.
- Liquid phase: $\eta^w = nS_w$, being $S_w = dv^w/(dv^w + dv^g + dv^\pi)$ the water saturation degree.
- Gaseous phase: $\eta^g = nS_g$, being $S_g = dv^g/(dv^w + dv^g + dv^\pi)$ the air saturation degree.
- Pollutant phase: $\eta^\pi = nS_\pi$, being $S_\pi = dv^\pi/(dv^w + dv^g + dv^\pi)$ the pollutant saturation degree.

The aforesaid equations yields:

$$S_w + S_g + S_\pi = 1 \tag{1}$$

and the multiphase media density is given by

$$\rho = \rho_s + \rho_w + \rho_g + \rho_\pi = (1 - n)\rho^s + nS_w\rho^w + nS_g\rho^g + nS_\pi\rho^\pi \tag{2}$$

Within this condition, and provided that the medium is constituted by different phases, any of them may be described relatively to any other previously defined, for example the solid phase. Thereby, relative velocities of the liquid, gaseous and pollutant may be addressed as follows:

$$\boldsymbol{v}^{ws} = \boldsymbol{v}^w - \boldsymbol{v}^s, \quad \boldsymbol{v}^{gs} = \boldsymbol{v}^g - \boldsymbol{v}^s, \quad \boldsymbol{v}^{\pi s} = \boldsymbol{v}^\pi - \boldsymbol{v}^s \tag{3}$$

3. Governing equations

3.1. Microscopic balance equations

The classical continuum mechanic balance equations will be taken into account in order to obtain the microscopic behaviour of an individual phase. For any thermodynamic attribute ψ, the general conservation equation for a single phase may be written as follows:

$$\frac{\partial \rho\psi}{\partial t} + \operatorname{div}(\rho\psi\dot{\boldsymbol{r}}) - \operatorname{div}\boldsymbol{i} - \rho\,\boldsymbol{b} = \rho\,\boldsymbol{G} \tag{4}$$

where $\dot{\boldsymbol{r}}$ is the phase local velocity in a fixed spatial point, ρ is the density, $\boldsymbol{b}$ is the external supply, $\boldsymbol{i}$ is the associated flux vector and $\boldsymbol{G}$ is the internal net production of ψ.

To set up balance equations for a certain thermodynamic attribute, ψ and the state variables $\boldsymbol{i}$, $\boldsymbol{b}$ and $\boldsymbol{G}$ must been alternatively modified. For the specific case of the mass balance equation they are given by:

$$\psi = 1; \quad \boldsymbol{i} = 0; \quad \boldsymbol{b} = 0; \quad \boldsymbol{G} = 0 \tag{5}$$

Introducing these values in Eq. (4), the microscopic mass balance equation is given by:

$$\frac{\partial \rho}{\partial t} + \operatorname{div}(\rho\dot{\boldsymbol{r}}) = 0 \tag{6}$$

3.2. Macroscopic balance equations

The macroscopic balance equations are obtained by the systematic application of the pioneer work of Hassanizadeh and Gray [9] to the microscopic balance equation, Eq. (4), in which for each constituent, the thermodynamic variable is substituted by the appropriate microscopic property [15]. The pollutant behaviour may be depicted in two different forms, depending on its mixing capability with the fluid or with the gaseous phase. In the most general situation, i.e., with immiscible pollutants, the behaviour may be described as another fluid phase, whereas with a soluble pollutant, three possible transport processes must be considered: advection, diffusion and dispersion.

3.2.1. Solid phase

From Eq. (6) and recalling the material time derivative of any differentiable function f^α, given in its spatial description and refering to a moving particle of the α phase,

$$\frac{\partial^\upsilon f^\alpha}{\partial t} = \frac{\partial^\alpha f^\alpha}{\partial t} + \operatorname{grad} f^\alpha \cdot \boldsymbol{v}^{\upsilon\alpha} \tag{7}$$

the mass balance expression for the solid phase is obtained:

$$\frac{\partial^s \rho_s}{\partial t} + \rho_s \operatorname{div} \boldsymbol{v}^s = 0 \tag{8}$$

where $\boldsymbol{v}^s$ is the solid skeleton velocity and

$$\operatorname{div}(\rho_s \boldsymbol{v}^s) = \rho_s \operatorname{div} \boldsymbol{v}^s + \operatorname{grad} \rho_s \cdot \boldsymbol{v}^s \tag{9}$$

Taking into account Eqs. (2) and (9), it is obtained:

$$\frac{(1-n)}{\rho^s}\frac{\partial^s \rho^s}{\partial t} - \frac{\partial^s n}{\partial t} + (1-n)\operatorname{div} \boldsymbol{v}^s = 0 \tag{10}$$

3.2.2. Liquid phase

The microscopic mass balance equation for the liquid phase is tantamount to the corresponding one for the solid phase being $\boldsymbol{G} \neq 0$ due to the possibility of transforming water into vapour and conversely.

Then, taking into account Eq. (6), with $\rho \boldsymbol{G} = -\dot{\boldsymbol{m}}$ in Eq. (5), the following expression is obtained:

$$\frac{\partial^w \rho_w}{\partial t} + \rho_w \operatorname{div} \boldsymbol{v}^w = -\dot{\boldsymbol{m}} \tag{11}$$

where $\boldsymbol{v}^w$ is the liquid phase mass velocity and $-\dot{\boldsymbol{m}}$ is the amount of water per unit volume transformed into vapour. Taking into account Eq. (2), it leads us to:

$$\frac{\partial (n S_w \rho^w)}{\partial t} + n S_w \rho^w \operatorname{div} \boldsymbol{v}^w = -\dot{\boldsymbol{m}} \tag{12}$$

Working with the above expression, after some algebra, considering Eqs. (3), (7) and (9) and adding the result to Eq. (10), the following expression is arrived:

$$\frac{(1-n)}{\rho^s}\frac{\partial^s \rho^s}{\partial t} + \operatorname{div} \boldsymbol{v}^s + \frac{n}{\rho^w}\frac{\partial^s \rho^w}{\partial t} + \frac{n}{S_w}\frac{\partial^s S_w}{\partial t} + \frac{1}{S_w \rho^w}\operatorname{div}(n S_w \rho^w \cdot \boldsymbol{v}^{ws}) = -\frac{\dot{\boldsymbol{m}}}{S_w \rho^w} \tag{13}$$

3.2.3. Gaseous phase

The gaseous phase is considered as composed by two constituents: dry air (ga) and water vapour (gw). Since both elements are miscible and their physical behaviour are similar, they may be treated as a single phase occupying the same differential volume, nS_g. Regardless of the internal mass production due to self-chemical reactions, the microscopic balance equation for this phase is once more given by Eq. (6).

$$\frac{\partial}{\partial t}(n S_g \rho^{ga}) + \operatorname{div}(n S_g \rho^{ga} \boldsymbol{v}^{ga}) = 0 \tag{14}$$

Likewise, making use of the gw superscript, the vapour balance equation is obtained:

$$\frac{\partial}{\partial t}(n S_g \rho^{gw}) + \operatorname{div}(n S_g \rho^{gw} \boldsymbol{v}^{gw}) = \dot{\boldsymbol{m}} \tag{15}$$

Clearly, given expressions (14) and (15), the mass balance equation for the dry air and water vapour mixture will be:

$$\frac{\partial}{\partial t}(n S_g \rho^g) + \operatorname{div}(n S_g \rho^g \boldsymbol{v}^g) = \dot{\boldsymbol{m}} \tag{16}$$

with $\rho^g = \rho^{ga} + \rho^{gw}$ and $\boldsymbol{v}^g = 1/\rho^g(\rho^{ga}\boldsymbol{v}^{ga} + \rho^{gw}\boldsymbol{v}^{gw})$.

Working with Eq. (16), a similar expression to Eq. (12) is obtained:

$$\frac{\partial^g (n S_g \rho^g)}{\partial t} + n S_g \rho^g \operatorname{div} \boldsymbol{v}^g = \dot{\boldsymbol{m}} \tag{17}$$

Once more, after some algebraic manipulation of the above expression, taking into account Eqs. (3), (7) and (9) and adding the remainder to Eq. (10), the subsequent relationship is arrived:

$$\frac{(1-n)}{\rho^s}\frac{\partial^s \rho^s}{\partial t} + \operatorname{div} \boldsymbol{v}^s + \frac{n}{S_g}\frac{\partial^s S_g}{\partial t} + \frac{n}{\rho^g}\frac{\partial^s \rho^g}{\partial t} + \frac{1}{S_g \rho^g}\operatorname{div}(n S_g \rho^g \cdot \boldsymbol{v}^{gs}) = \frac{\dot{\boldsymbol{m}}}{S_g \rho^g} \tag{18}$$

3.2.4. Immiscible pollutant

When the pollutant existing in the porous media has no miscible property with any of the non-solids phases, it is clearly taking part of a new phase, π. One way to handle with this phenomenon is to consider the pollutant behaviour similar to the liquid phase [20], whereby it is possible to yield the conservation equations for the pollutant as it was done for the liquid phase. Therefore, the mass balance equation for immiscible pollutants will be likewise Eq. (13), but without the internal production term (source), i.e., $\dot{\boldsymbol{m}} = 0$.

$$\frac{(1-n)}{\rho^s}\frac{\partial^s \rho^s}{\partial t} + \operatorname{div} \boldsymbol{v}^s + \frac{n}{\rho^\pi}\frac{\partial^s \rho^\pi}{\partial t} + \frac{n}{S_\pi}\frac{\partial^s S_\pi}{\partial t} + \frac{1}{S_\pi \rho^\pi}\operatorname{div}(n S_\pi \rho^\pi \cdot \boldsymbol{v}^{\pi s}) = 0 \tag{19}$$

From now on, if no extra explanation is given, all time derivatives will be following the solid phase.

3.3. Constitutive and state relationships

To provide a complete description of the mechanical behaviour, constitutive equations are required. The balance equations developed in the previous section take into account elaborate constitutive theories, especially when these equations are valid at the interfaces [9].

3.3.1. Fluid phase stress tensor

By the application of the second law of thermodynamics to the porous media [8], the stress tensor for the fluid phase may be written as

$$\boldsymbol{t}^\gamma = -\eta^\gamma p^\gamma \mathbf{I} \tag{20}$$

being $\mathbf{I}$ the unit tensor, p^γ is pressure of the phase γ and η^γ is the phase volume fraction of the same phase. It may be clearly noticed that no deviatoric stresses are present in the fluid phase stress tensor.

3.3.2. Solid phase stress tensor

As in the previous section, by means of the use of the second law of thermodynamics for the porous media [9], the stress tensor for the solid phase is given by

$$\boldsymbol{t}^s = (1-n)(\boldsymbol{t}_e^s - \boldsymbol{I}\, p^s) \tag{21}$$

while the solid phase pressure and the effective stress tensor are, respectively, expressed by:

$$p^s = S_w p^w + S_g p^g + S_\pi p^\pi \tag{22}$$

and

$$\boldsymbol{\sigma}' = (1-n)\boldsymbol{t}_e^s \tag{23}$$

Introducing Eq. (22) in Eq. (21), the following expression for the solid phase stress tensor is obtained:

$$\boldsymbol{t}^s = (1-n)[\boldsymbol{t}_e^s - \mathbf{I}(S_w p^w + S_g p^g + S_\pi p^\pi)] \tag{24}$$

The volume fraction $(1-n)$ points out that $\boldsymbol{t}^s$ is the stress exerted over the solid phase. In order to obtain the total stress, $\boldsymbol{\sigma}$, the expressions derived for the liquid and the gaseous phases in Eq. (24) must be added to Eq. (20), giving:

$$\begin{aligned}\boldsymbol{\sigma} &= \boldsymbol{t}^s + \boldsymbol{t}^w + \boldsymbol{t}^g + \boldsymbol{t}^\pi = (1-n)[\boldsymbol{t}_e^s - \mathbf{I}(S_w p^w + S_g p^g + S_\pi p^\pi)] - n S_w p^w \mathbf{I} - n S_g p^g \mathbf{I} - n S_\pi p^\pi \mathbf{I} \\ &= (1-n)\boldsymbol{t}_e^s - \mathbf{I}(S_w p^w + S_g p^g + S_\pi p^\pi)\end{aligned} \tag{25}$$

Eq. (25) may be arranged in order to obtain the most well known form in soil mechanics [13]:

$$\boldsymbol{\sigma} = \boldsymbol{\sigma}' + \mathbf{I}(p^w S_w + p^g S_g + p^\pi S_\pi) \tag{26}$$

3.3.3. Solid mass density

Considering a compressible solid mass, an expression for the time derivative of the solid mass density may be obtained from the mass conservation differential equation

$$\frac{\partial^s(\rho^s V^s)}{\partial t} = 0 \tag{27}$$

Assuming that the solid mass density is function of p^s, Eq. (22), of the temperature and of the first effective stress tensor invariant, it is obatined:

$$\frac{1}{\rho^s}\frac{\partial^s \rho^s}{\partial t} = -\frac{1}{V_s}\frac{\partial^s V_s}{\partial t} = \frac{1}{K_s}\frac{\partial^s p^s}{\partial t} - \beta_s \frac{\partial^s T}{\partial t} - \frac{1}{3(n-1)K_s}\frac{\partial^s (\mathrm{tr}\boldsymbol{\sigma}')}{\partial t} \tag{28}$$

where the following expressions were regarded:

$$\frac{1}{\rho^s}\frac{\partial^s \rho^s}{\partial p^s} = \frac{1}{K_s} \tag{29}$$

$$\frac{1}{\rho^s}\frac{\partial^s \rho^s}{\partial T} = -\beta_s \tag{30}$$

$$\frac{1}{\rho^s}\frac{\partial^s \rho^s}{\partial (\mathrm{tr}\boldsymbol{\sigma}')} = -\frac{1}{3(n-1)K_s} \tag{31}$$

being, K_s the grain compressibility coefficient, β_s the grain thermal expansion and $\mathrm{tr}\boldsymbol{\sigma}'$ the first invariant of the stress tensor. Having in mind the constitutive relationship for the first invariant of the effective stress tensor, the following expression is valid:

$$\frac{\partial^s \mathrm{tr}\boldsymbol{\sigma}'}{\partial t} = 3K_T\left(\mathrm{div}\boldsymbol{v}^s + \frac{1}{K_s}\frac{\partial^s p^s}{\partial t} - \beta_s \frac{\partial^s T}{\partial t}\right) \tag{32}$$

where, K_T, is the skeleton bulk modulus. Considering the Biot constant definition [2], given by:

$$1 - \alpha = \frac{K_T}{K_s} \tag{33}$$

and expressions (32) and (28), it is obtained:

$$\frac{1}{\rho^s}\frac{\partial^s \rho^s}{\partial t} = \frac{1}{1-n}\left[(\alpha - n)\frac{1}{K_s}\frac{\partial^s p^s}{\partial t} - \beta_s(\alpha - n)\frac{\partial^s T}{\partial t} - (1-\alpha)\,\mathrm{div}\,\boldsymbol{v}^s\right] \tag{34}$$

The incompressible grain condition, i.e., $1/K_s = 0$ and $\alpha = 1$, do not indicate whatsoever a rigid or incompressible skeleton, since under load application, an interstitial voids re-arrangements is undertaken.

3.3.4. State equation for the liquid phase

The water solid state equation was developed by Murty et al. [18] and it is given by:

$$\rho^w = \rho^{wo}\exp[-\beta_w T + C_w(p^w - p^{wo})] \tag{35}$$

where the superscript o stands for the initial state, β_w is the thermal expansion coefficient and C_w is the compressibility coefficient. Taking the series expansion of Eq. (20) and disregarding the higher order terms, it is obtained

$$\rho^w = \rho^{wo}[1 - \beta_w T + C_w(p^w - p^{wo})] \tag{36}$$

being the time derivative given by:

$$\frac{1}{\rho^{wo}}\frac{\partial^w \rho^w}{\partial t} = \frac{1}{K_w}\frac{\partial^w p^w}{\partial t} - \beta_w \frac{\partial^w T}{\partial t} \tag{37}$$

where $K_w = 1/C_w$ is the water bulk modulus. Eq. (37) may be also obtained from the mass balance differential equation [15].

3.3.5. State equation for the gaseous phase

The gaseous phase may be considered as a mixture of perfect ideal gases, dry air and water vapour. Therefore, it is possible to apply the ideal gas laws by relating the constituent partial pressure (p^{ga} or p^{gw}), the constituent mass concentration in the gaseous phase (ρ^{ga} or ρ^{gw}) and the absolute temperature T. The perfect gas state equations applied to dry air (ga), to water vapour (qw) and to the air (g), are [5]:

$$p^{ga} = \frac{\rho^{ga} TR}{M_a} \tag{38}$$

$$p^{gw} = \frac{\rho^{gw} TR}{M_w} \tag{39}$$

$$\rho^{g} = \rho^{ga} + \rho^{gw} \tag{40}$$

$$p^{g} = p^{ga} + p^{gw} \tag{41}$$

$$M_g = \left(\frac{\rho^{gw}}{\rho^{g}} \frac{1}{M_w} + \frac{\rho^{ga}}{\rho^{g}} \frac{1}{M_a} \right)^{-1} \tag{42}$$

where M_i is the molar mass of the i constituent and R is the universal gas constant.

3.3.6. Pollutant saturation–suction coupling effects

Earlier FE models for non-saturated soils [11] did not consider the saturation degree variation with time, leading to symmetric equations systems. Therefore, this situation motivate many authors [6] to study the behaviour of partially saturated soils, and a relationship between the water saturation degree, S^w, and the suction, $p^{gw} = p^g - p^w$,was settled down. This relationship is referred as the soil–water characteristic curve.

The mathematical models that involve the saturation–suction coupling effects and, consequently, based on these curves [15,17], lead to accurate soil deformation prediction when they are checked against experimental results. However, the symmetry presented in the former case is lost, yielding to additional costs in terms of processing time and computational memory.

Di Rado et al. [4] proposed a non-saturated soil model leading to a flexible system of equation that may be treated alternatively as symmetrical or non-symmetrical, according to the relevance of the saturation–suction coupling effects, which relevance is assessed based on saturation values and the slope of the saturation–suction curve.

Due to the existence of immiscible substances in the soil, the three-phase system considered by Di Rado et al. [4] becomes a multiphase system and thereby, a new suction relationship arises, namely $p^{g\pi} = p^g - p^\pi$, being p^π the pollutant pore pressure.

The new phases behave similar to the liquid phase in many aspects, even though they are not equal. Among others issues, a different definition for the saturation–suction relationship $S_\pi - p^{g\pi}$ is demanded. Hence, for this work, the following expression was adopted:

$$S_\pi = SB - (SB - MB)\tanh(LB\, p^{g\pi}) \tag{43}$$

where SB, MB and LB are shape parameters. It allows to model different configurations for the saturation–suction curve likewise the soil–water characteristic curve, proposed by Fredlund and Xing [6] (see Fig. 2), with an additional important property: expression (43) can be easily inverted, and no further algorithm for the solution of the root function when the suction value is entailed for a certain saturation degree, is required.

4. General field equations

Macroscopic balance laws are currently transformed by the introduction of the constitutive relationships previously defined in Section 3.3.

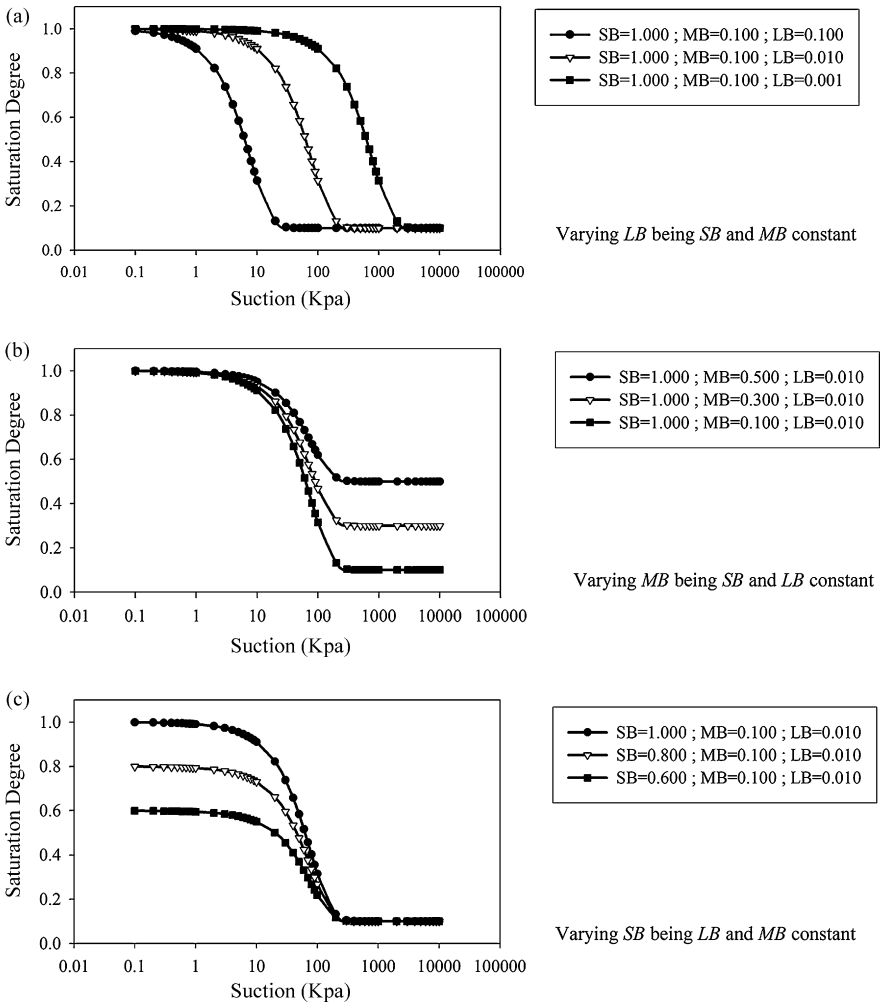

Fig. 2. Curve $S_\pi - p^{g\pi}$: possible configurations with respect to shape parameters *SB*, *MB* and *LB*; (a) varying *LB*, being *SB* and *MB* constant; (b) varying *MB*, being *SB* and *LB* constant; (c) varying *SB*, being *LB* and *MB* constant.

4.1. Solid phase

The solid phase behaviour may be conveniently depicted using the lineal momentum balance equation, which is obtained from Eq. (4) by appropriately setting the state variables $\boldsymbol{i}$, $\boldsymbol{b}$ and $\boldsymbol{G}$ [15].

$$\mathbf{L}^T\boldsymbol{\sigma} + \rho\boldsymbol{g} = 0 \tag{44}$$

where $\boldsymbol{g}$ is the gravity acceleration and the differential operator is given by:

$$\mathbf{L}^T = \begin{vmatrix} \partial/\partial x & 0 & 0 & \partial/\partial y & 0 & \partial/\partial z \\ 0 & \partial/\partial y & 0 & \partial/\partial x & \partial/\partial z & 0 \\ 0 & 0 & \partial/\partial z & 0 & \partial/\partial y & \partial/\partial x \end{vmatrix} \tag{45}$$

4.2. Liquid phase

Taking the derivative of the saturation degree of the different phases given in Eq. (1) with respect to time and clearing $\partial S_g/\partial t$, it is obtained:

$$\frac{\partial S_g}{\partial t} = -\frac{\partial S_w}{\partial t} - \frac{\partial S_\pi}{\partial t} \tag{46}$$

Introducing the liquid phase state, Eq. (37), the solid phase pressure definition, Eq. (22), and the solid phase density, Eq. (34), in the macroscopic balance of the liquid phase, Eq. (13), and constraining the problem to an isothermal condition, the following expression is obtained:

$$\begin{aligned}
&\left[S_w^2\frac{\alpha-n}{K_s} + \frac{nS_w}{K_w}\right]\frac{\partial p^w}{\partial t} + \left[\frac{\alpha-n}{K_s}S_wS_g\right]\frac{\partial p^g}{\partial t} + \left[\frac{\alpha-n}{K_s}S_wS_\pi\right]\frac{\partial p^\pi}{\partial t}\\
&+\alpha\, S_w m^T\mathbf{L}\frac{\partial u}{\partial t} + \left[\frac{\alpha-n}{K_s}S_w p^w - \frac{\alpha-n}{K_s}S_w p^g + n\right]\frac{\partial S_w}{\partial t} + S_w\frac{\alpha-n}{K_s}\left[p^\pi - p^g\right]\frac{\partial S_\pi}{\partial t}\\
&+\frac{1}{\rho^w}\nabla^T\left[\frac{kk^{rw}}{\mu^w}(-\nabla p^w + \rho^w g)\right] = 0
\end{aligned} \tag{47}$$

Terms like $\partial S_w/\partial t$ and $\partial S_\pi/\partial t$ may be written as follows

$$\begin{aligned}
n\frac{\partial S_w}{\partial t} &= n\frac{\partial S_w}{\partial p^{gw}}\frac{\partial p^{gw}}{\partial t} = C_w\frac{\partial p^{gw}}{\partial t} = C_w\left(\frac{\partial p^g}{\partial t} - \frac{\partial p^w}{\partial t}\right)\\
n\frac{\partial S_\pi}{\partial t} &= n\frac{\partial S_\pi}{\partial p^{g\pi}}\frac{\partial p^{g\pi}}{\partial t} = C_\pi\frac{\partial p^{g\pi}}{\partial t} = C_\pi\left(\frac{\partial p^g}{\partial t} - \frac{\partial p^\pi}{\partial t}\right)
\end{aligned} \tag{48}$$

where $n\partial S_w/\partial p^{gw} = C_w$ is the derivative of the water saturation with respect to the suction, which may be obtained with the aid of the soil characteristic curve ($S_w - p^{gw}$) [4,6]. Since the π phase behaves like a fluid, an equivalent analysis may be achieved by the mere implementation of a new $S_\pi - p^{g\pi}$ curve which allows the assessment of the derivative $n\,\partial S_\pi/\partial p^{g\pi} = C_\pi$ as it was done for the water phase [19]. One possibility is the adoption of a hyperbolic function [3] for the above mentioned $S_\pi - p^{g\pi}$ curve.

Taking into account Eqs. (47) and (48), the following expression is obtained:

$$\alpha_{22}\frac{\partial p^w}{\partial t} + \alpha_{23}\frac{\partial p^g}{\partial t} + \alpha_{24}\frac{\partial p^\pi}{\partial t} + \alpha_{21}\mathbf{L}\frac{\partial u}{\partial t} + \frac{1}{\rho^w}\nabla^T\left[\frac{kk^{rw}}{\mu^w}(-\nabla p^w + \rho^w g)\right] = 0 \tag{49}$$

with

$$\begin{aligned}
\alpha_{21} &= \alpha\, S_w m^T\\
\alpha_{22} &= \frac{\alpha-n}{K_s}S_w\left(S_w - p^w\frac{C_w}{n} + p^g\frac{C_w}{n}\right) + \frac{nS_w}{K_w} - C_w\\
\alpha_{23} &= \frac{\alpha-n}{K_s}S_w\left(S_g + p^w\frac{C_w}{n} - p^g\frac{C_w}{n} + (p^\pi - p^g)\frac{C_\pi}{n}\right) + C_w\\
\alpha_{24} &= \frac{\alpha-n}{K_s}S_w\left(S_\pi - (p^\pi - p^g)\frac{C_\pi}{n}\right).
\end{aligned} \tag{50}$$

4.3. Gaseous phase

From the gaseous phase balance equation for isothermal processes, Eq. (18), and regarding the state equation for the gaseous phase, Eq. (42), the relative velocity definition, Eq. (3), the solid phase density, Eq. (34) and Eqs. (46) and (48), the following mathematical statement is obtained:

$$\left[\frac{\alpha-n}{K_s}S_g\left(S_w-\frac{C_w}{n}(p^w-p^g)\right)+C_w\right]\frac{\partial p^w}{\partial t}$$
$$+\left[\frac{\alpha-n}{K_s}S_g\left(S_g+\frac{C_w}{n}(p^w-p^g)+\frac{C_\pi}{n}(p^\pi-p^g)\right)-C_w-C_\pi+\frac{nS_gM_g}{\rho^gTR}\right]\frac{\partial p^g}{\partial t}$$
$$+\left[\frac{\alpha-n}{K_s}S_g\left(S_\pi-\frac{C_\pi}{n}(p^\pi-p^g)\right)+C_\pi\right]\frac{\partial p^\pi}{\partial t}+\alpha S_g\, m^T\mathbf{L}\frac{\partial u}{\partial t}+\frac{1}{\rho^g}\nabla^T\left[\frac{kk^{rg}}{\mu^g}(-\nabla p^g+\rho^g g)\right]=0 \quad (51)$$

which may be written similarly to Eq. (49) as follows:

$$\alpha_{32}\frac{\partial p^w}{\partial t}+\alpha_{33}\frac{\partial p^g}{\partial t}+\alpha_{34}\frac{\partial p^\pi}{\partial t}+\alpha_{31}\mathbf{L}\frac{\partial u}{\partial t}+\frac{1}{\rho^g}\nabla^T\left[\frac{kk^{rg}}{\mu^g}(-\nabla p^g+\rho^g g)\right]=0 \quad (52)$$

with

$$\begin{aligned}
\alpha_{31}&=\alpha S_g\, m^T\\
\alpha_{32}&=\frac{\alpha-n}{K_s}S_g\left(S_w+\frac{C_w}{n}(p^g-p^w)\right)+C_w\\
\alpha_{33}&=\frac{\alpha-n}{K_s}S_g\left(S_g-\frac{C_w}{n}(p^g-p^w)-\frac{C_\pi}{n}(p^g-p^\pi)\right)-C_w-C_\pi+\frac{nS_gM_g}{\rho^gTR}\\
\alpha_{34}&=\frac{\alpha-n}{K_s}S_g\left(S_\pi+\frac{C_\pi}{n}(p^g-p^\pi)\right)+C_\pi
\end{aligned} \quad (53)$$

4.4. Immiscible pollutant phase

Whenever the pollutant is unable to mix with the liquid phase and accordingly to what was settled herein, it is clearly forming a new phase, π. The mathematical framework may be stated likewise the liquid phase [20]. From the immiscible pollutant mass balance equation for isothermal processes, Eq. (19), and regarding expressions (34), (37), (46) and (48), it is obtained:

$$\left[\frac{\alpha-n}{K_s}S_\pi\left[S_w-(p^w-p^g)\frac{C_w}{n}\right]\right]\frac{\partial p^w}{\partial t}+\left[\frac{\alpha-n}{K_s}S_\pi\left[S_g+(p^w-p^g)\frac{C_w}{n}+(p^\pi-p^g)\frac{C_\pi}{n}\right]+C_\pi\right]\frac{\partial p^g}{\partial t}$$
$$+\left[\frac{\alpha-n}{K_s}S_\pi\left[S_\pi-(p^\pi-p^g)\frac{C_\pi}{n}\right]+\frac{nS_\pi}{K_\pi}-C_\pi\right]\frac{\partial p^\pi}{\partial t}+\alpha\, S_\pi m^T\mathbf{L}\frac{\partial u}{\partial t}+\frac{1}{\rho^\pi}\nabla^T\left[\frac{kk^{r\pi}}{\mu^\pi}(-\nabla p^\pi+\rho^\pi g)\right]=0 \quad (54)$$

which may be expressed likewise Eq. (49) as follows:

$$\alpha_{42}\frac{\partial p^w}{\partial t}+\alpha_{43}\frac{\partial p^g}{\partial t}+\alpha_{44}\frac{\partial p^\pi}{\partial t}+\alpha_{41}\mathbf{L}\frac{\partial u}{\partial t}+\frac{1}{\rho^\pi}\nabla^T\left[\frac{kk^{r\pi}}{\mu^\pi}(-\nabla p^\pi+\rho^\pi g)\right]=0 \quad (55)$$

with

$$\begin{aligned}
\alpha_{41}&=\alpha\, S_\pi m^T\\
\alpha_{42}&=\frac{\alpha-n}{K_s}S_\pi\left[S_w-(p^w-p^g)\frac{C_w}{n}\right]\\
\alpha_{43}&=\frac{\alpha-n}{K_s}S_\pi\left[S_g+(p^w-p^g)\frac{C_w}{n}+\left(p^\pi-p^g\right)\frac{C_\pi}{n}\right]+C_\pi\\
\alpha_{44}&=\frac{\alpha-n}{K_s}S_\pi\left[S_\pi-(p^\pi-p^g)\frac{C_\pi}{n}\right]+\frac{nS_\pi}{K_\pi}-C_\pi
\end{aligned} \quad (56)$$

5. Discrete mathematical model

By the application of Galerkin method to the differential system of equations described by Eqs. (44), (49), (52) and (55), and discretizing using the FE method, the following ordinary differential equations system (ODES) is furnished:

$$\boldsymbol{K}_E \frac{\partial \bar{\boldsymbol{u}}}{\partial t} + \boldsymbol{C}_{sw} \frac{\partial \bar{p}^w}{\partial t} + \boldsymbol{C}_{sg} \frac{\partial \bar{p}^g}{\partial t} + \boldsymbol{C}_{s\pi} \frac{\partial \bar{p}^\pi}{\partial t} = \frac{\partial \boldsymbol{f}^u}{\partial t} \tag{57}$$

$$\boldsymbol{P}_{ww} \frac{\partial \bar{p}^w}{\partial t} + \boldsymbol{C}_{wg} \frac{\partial \bar{p}^g}{\partial t} + \boldsymbol{C}_{w\pi} \frac{\partial \bar{p}^\pi}{\partial t} + \boldsymbol{C}_{ws} \frac{\partial \bar{\boldsymbol{u}}}{\partial t} + \boldsymbol{H}_{ww} \bar{p}^w = \boldsymbol{f}^w \tag{58}$$

$$\boldsymbol{C}_{gw} \frac{\partial \bar{p}^w}{\partial t} + \boldsymbol{P}_{gg} \frac{\partial \bar{p}^g}{\partial t} + \boldsymbol{C}_{g\pi} \frac{\partial \bar{p}^\pi}{\partial t} + \boldsymbol{C}_{gs} \frac{\partial \bar{\boldsymbol{u}}}{\partial t} + \boldsymbol{H}_{gg} \bar{p}^g = \boldsymbol{f}^g \tag{59}$$

$$\boldsymbol{C}_{\pi w} \frac{\partial \bar{p}^w}{\partial t} + \boldsymbol{C}_{\pi g} \frac{\partial \bar{p}^g}{\partial t} + \boldsymbol{P}_{\pi\pi} \frac{\partial \bar{p}^\pi}{\partial t} + \boldsymbol{C}_{\pi s} \frac{\partial \bar{\boldsymbol{u}}}{\partial t} + \boldsymbol{H}_{\pi\pi} \bar{p}^\pi = \boldsymbol{f}^\pi \tag{60}$$

Eqs. (57)–(60) may be written using a matrix description, giving the following expression:

$$\begin{bmatrix} \boldsymbol{K}_E & \boldsymbol{C}_{sw} & \boldsymbol{C}_{sg} & \boldsymbol{C}_{s\pi} \\ \boldsymbol{C}_{ws} & \boldsymbol{P}_{ww} & \boldsymbol{C}_{wg} & \boldsymbol{C}_{w\pi} \\ \boldsymbol{C}_{gs} & \boldsymbol{C}_{gw} & \boldsymbol{P}_{gg} & \boldsymbol{C}_{g\pi} \\ \boldsymbol{C}_{\pi s} & \boldsymbol{C}_{\pi w} & \boldsymbol{C}_{\pi g} & \boldsymbol{P}_{\pi\pi} \end{bmatrix} \begin{bmatrix} \dot{\bar{\boldsymbol{u}}} \\ \dot{\bar{p}}^w \\ \dot{\bar{p}}^g \\ \dot{\bar{p}}^\pi \end{bmatrix} + \begin{bmatrix} 0 & 0 & 0 & 0 \\ 0 & \boldsymbol{H}_{ww} & 0 & 0 \\ 0 & 0 & \boldsymbol{H}_{gg} & 0 \\ 0 & 0 & 0 & \boldsymbol{H}_{\pi\pi} \end{bmatrix} \begin{bmatrix} \bar{\boldsymbol{u}} \\ \bar{p}^w \\ \bar{p}^g \\ \bar{p}^\pi \end{bmatrix} = \begin{bmatrix} \dot{\boldsymbol{f}}^u \\ \boldsymbol{f}^w \\ \boldsymbol{f}^g \\ \boldsymbol{f}^\pi \end{bmatrix} \tag{61}$$

All matrices and vectors are presented in Appendix A.

6. Numerical examples

6.1. Unidimensional soil column problem

In first place, an example for the validation of the mathematical model addresed in the present work is suggested. The outcomes obtained in this work from the FE simulation were checked against experimental results presented in Lewis et al. [14] as well as against the numerical results for the situation without pollutant presence presented in Di Rado et al. [4].

The soil column was assumed to be unsaturated with initial water saturation S_w equal to 0.52. The initial pore water pressure was taken equal to −280 kpa and the boundary pore water pressure was instantaneously changed to −420 kpa at the surface. Furthermore, the constitutive behavior of the solid phase is assumed elastic.

The FE mesh and boundary conditions are shown in Fig. 3. Biquadratic quadrilateral isoparametric elements (with 8 nodes) were adopted for the FE mesh. Moreover, the material parameters are: wide $B = 0.10$ m; height $H = 1.00$ m; Young's modulus $E = 1.73 \times 10^5$ kpa; Poisson's ratio $\mu = 0.3$; initial void ratio $e_0 = 0.4$; vertical permeability coefficient $k_y = 0.11456$ m/day; water and pollutant compressibility coefficient $K_f = K_\pi = 4.3 \times 10^9$ kpa; grain compressibility $K_s = 1.4 \times 10^6$ kpa.

Fig. 4 shows the vertical displacements vs. time for a point located at half the height of the soil column (point A in Fig. 3). The cross symbols stands for a previous work presented by Lewis et al. [14], the dotted line and the solid line were used for the results addressed in Di Rado [4] and the results obtained here with null pollutant saturation, respectively. It may be straightforward noticed that the three mentioned plots agree with each other, allowing us to validate the mathematical simulation carried out in the present work. Furthermore, the vertical displacements vs. time for different pollutant saturation values were included as well.

6.2. One-dimensional multiphase soil consolidation problem

The following example consists in a non-saturated soil column with liquid and gaseous substances as well as another immiscible substance gathered in the solid skeleton voids. The sample may be treated as an one-dimensional model.

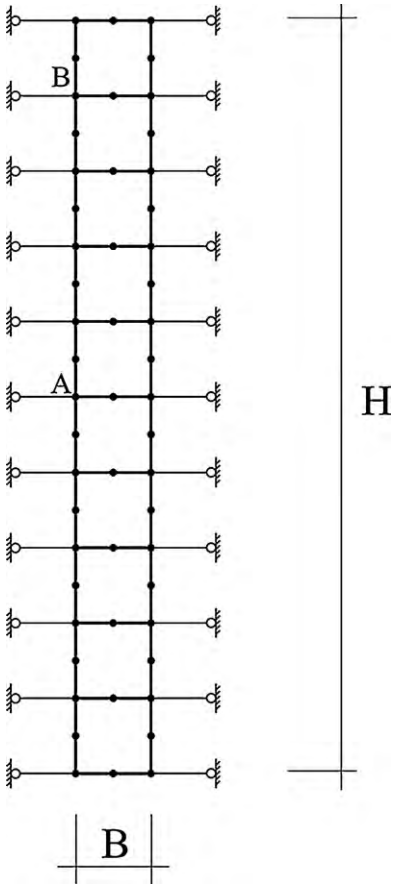

Fig. 3. FEM mesh and boundary conditions.

The physical and geometric data of the problem are given as follows: wide $B = 0.10$ m; height $H = 1.00$ m; load $q = 10.0$ kpa; Young's modulus $E = 1000.0$ kpa; Poisson's ratio $\mu = 0.3$; initial void ratio $e_0 = 2.0$; vertical permeability coefficient $k_y = 8.64 \times 10^{-3}$ m/day; water and pollutant compressibility coefficient $K_f = K_\pi = 1.0 \times 10^6$ kpa; initial water saturation degree $S_w = 0.50$; initial pollutant saturation degree $S_\pi = 0.40$. The pore pressures on the top sur-

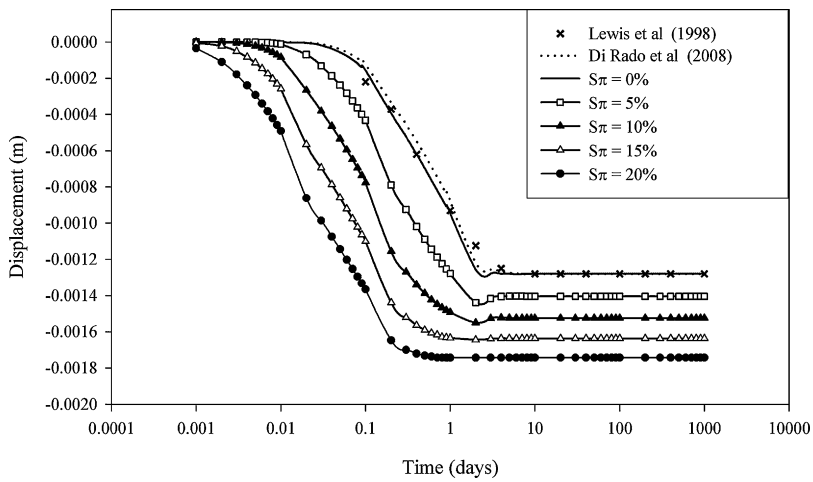

Fig. 4. Vertical displacements vs. time at point A, comparison against experimental data.

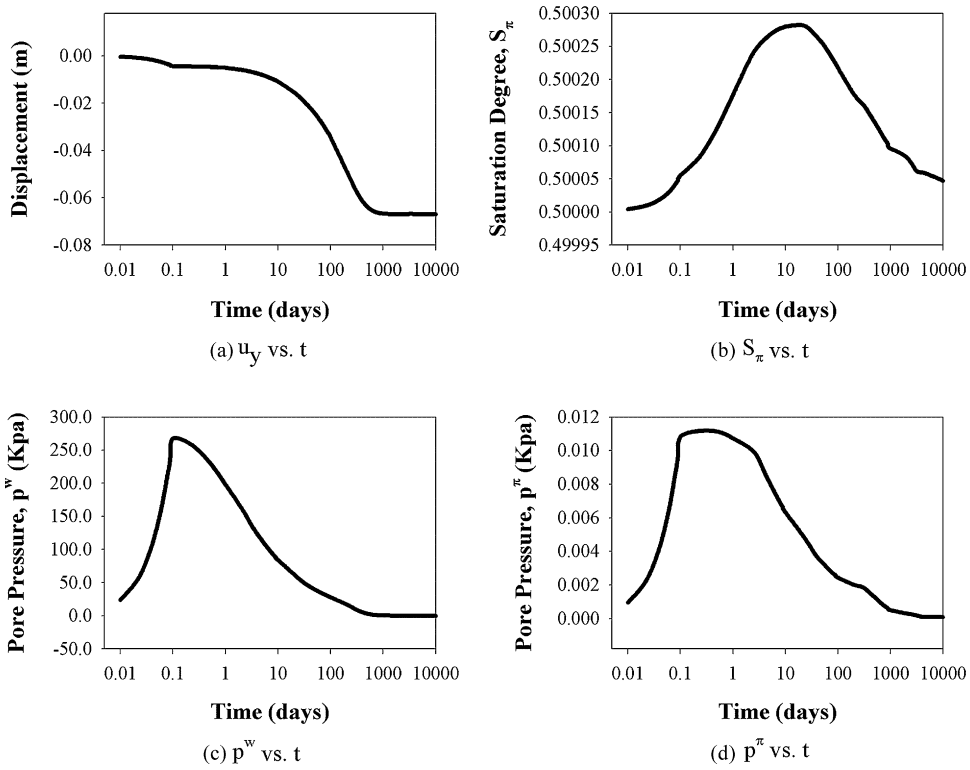

Fig. 5. One-dimensional soil column. Numerical results at point B of Fig. 3: (a) displacement vs. time; (b) pollutant saturation degree vs. time; (c) Water pore pressure vs. TIME; (d) pollutant pore pressure vs. time.

face are set to zero (atmospheric pressure), whereas the boundary conditions for displacements are indicated in Fig. 3.

In Fig. 5(a)–(d), plots standing for displacements vs. time (settlement evolution), the pollutant saturation vs. time as well as the pore water and pore pollutant values vs. time at point B of Fig. 3, were respectively presented.

A further discussion on the results shown in Fig. 5 allows pointing out that the pore pressure evolution is indeed in agreement with the solid phase deformation as well as with the saturation degree decrease due to the reduction of the interstitial voids with the load process evolution.

6.3. *Strip footing*

The following example models the two-dimensional consolidation problem in partially saturated soils with immiscible pollutant presence. It consists on a strip footing under uniform load, $q = 10$ kN/m, width $H = 2$ m and Depth $B = 4$ m.

Soil-type characteristics match those typically found in the Argentine Northeast region: Young's modulus $E = 1500.0$ kpa, Poisson's ratio $\mu = 0.3$, specific weight $\gamma = 19.61$ kN/m, initial void ratio $e_0 = 2.0$, grains compressibility $K_s = 1.0 \times 10^6$ kpa and permeability coefficient $k = 8.64 \times 10^{-4}$ m/day.

Boundary condition are summarized in Table 1; furthermore, the water and the pollutant saturation degree at the beginning of the load process are $S_w = 0.70$ and $S_\pi = 0.20$, respectively.

The FE mesh has 210 bilinear isoparametric quadrilateral elements. In Fig. 6, the displacement as well as the distorted FE mesh, is presented. Finally, Fig. 7 shows the water pore pressure distribution 7 (seven) h after load application on the left and 30 (thirty) h after load application on the right, respectively. Likewise, in Fig. 8, the pollutant pore pressure distribution at the same time steps is presented.

Table 1
Boundary conditions.

Boundary	*X*-Displa.	*Y*-Displa.	Water-Pres.	Air-Pres.	Pollutant-Pres.
A–B	Yes	No	No	No	No
B–C	No	Yes	No	No	No
C–D	Yes	No	No	No	No
D–E	No	No	Yes	Yes	Yes
F–A	No	No	Yes	Yes	Yes

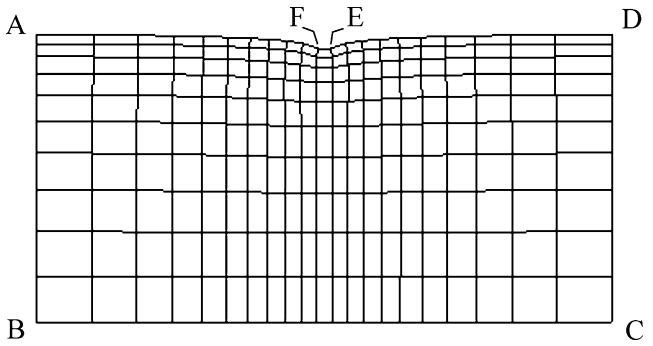

Fig. 6. FE mesh and deformed configuration.

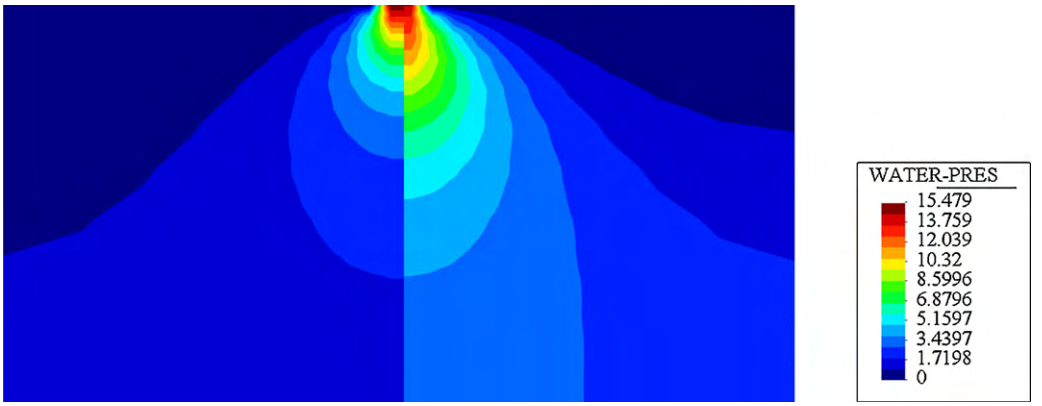

Fig. 7. Water pore pressure distribution at 7 h (on the left) and 30 h (on the right).

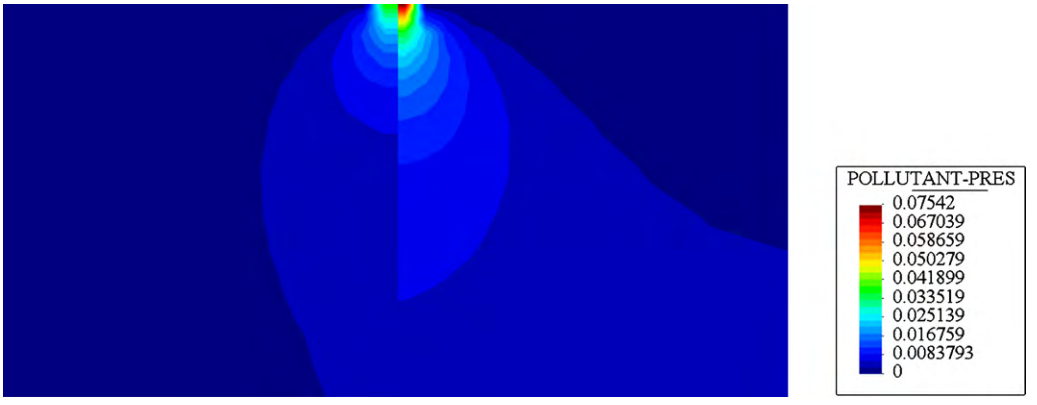

Fig. 8. Pollutant pore pressure distribution at 7 h (on the left) and 30 h (on the right).

7. Concluding remarks

A coupled mathematical framework for the solution of pore pressures and displacements of a non-saturated porous media with three fluid phases in isothermal conditions was presented. Furthermore, the solution of the aforementioned problem using the FE method was carried out. The previous model presented by the authors was widened including the pollutant phase as well as a specific suction–saturation relationship for the added constituent. Encouraging outcomes were obtained based on the general compatibility between the different variables values. Specifically, Fig. 4 shows that as long as the pollutant saturation decreases the vertical displacements declines as well. This situation arises due to the physical features that pollutants render to the whole system and due to a declination in the air saturation. At the limit situation, namely, when the saturation value tends to zero, the obtained displacements match perfectly the experimental results.

Appendix A.

In this appendix de FE matrices and vectors for the discrete mathematical model, corresponding to the ODES of Eq. (61) are presented

$$
\begin{aligned}
&\boldsymbol{K}_E = \int_\Omega \boldsymbol{B}^T \boldsymbol{D}_E \boldsymbol{B}\,\mathrm{d}\Omega \\
&\boldsymbol{C}_{sw} = \int_\Omega \boldsymbol{B}^T \alpha_{12} \boldsymbol{N}_p\,\mathrm{d}\Omega \quad \boldsymbol{C}_{ws} = \int_\Omega \boldsymbol{N}_u^T \alpha_{21} \boldsymbol{B}\,\mathrm{d}\Omega \\
&\boldsymbol{C}_{sg} = \int_\Omega \boldsymbol{B}^T \alpha_{13} \boldsymbol{N}_p\,\mathrm{d}\Omega \quad \boldsymbol{C}_{gs} = \int_\Omega \boldsymbol{N}_u^T \alpha_{31} \boldsymbol{B}\,\mathrm{d}\Omega \\
&\boldsymbol{C}_{s\pi} = \int_\Omega \boldsymbol{B}^T \alpha_{14} \boldsymbol{N}_p\,\mathrm{d}\Omega \quad \boldsymbol{C}_{\pi s} = \int_\Omega \boldsymbol{N}_u^T \alpha_{41} \boldsymbol{B}\,\mathrm{d}\Omega \\
&\boldsymbol{C}_{wg} = \int_\Omega \boldsymbol{N}_p^T \alpha_{23} \boldsymbol{N}_p\,\mathrm{d}\Omega \quad \boldsymbol{C}_{gw} = \int_\Omega \boldsymbol{N}_p^T \alpha_{32} \boldsymbol{N}_p\,\mathrm{d}\Omega \\
&\boldsymbol{C}_{w\pi} = \int_\Omega \boldsymbol{N}_p^T \alpha_{24} \boldsymbol{N}_p\,\mathrm{d}\Omega \quad \boldsymbol{C}_{\pi w} = \int_\Omega \boldsymbol{N}_p^T \alpha_{42} \boldsymbol{N}_p\,\mathrm{d}\Omega \\
&\boldsymbol{C}_{g\pi} = \int_\Omega \boldsymbol{N}_p^T \alpha_{34} \boldsymbol{N}_p\,\mathrm{d}\Omega \quad \boldsymbol{C}_{\pi g} = \int_\Omega \boldsymbol{N}_p^T \alpha_{43} \boldsymbol{N}_p\,\mathrm{d}\Omega \\
&\boldsymbol{P}_{ww} = \int_\Omega \boldsymbol{N}_p^T \alpha_{22} \boldsymbol{N}_p\,\mathrm{d}\Omega \quad \boldsymbol{P}_{gg} = \int_\Omega \boldsymbol{N}_p^T \alpha_{33} \boldsymbol{N}_p\,\mathrm{d}\Omega \\
&\boldsymbol{P}_{\pi\pi} = \int_\Omega \boldsymbol{N}_p^T \alpha_{44} \boldsymbol{N}_p\,\mathrm{d}\Omega
\end{aligned}
\tag{A.1}
$$

$$
\begin{aligned}
&\boldsymbol{H}_{ww} = \frac{1}{S_w \rho^w} \int_\Omega (\nabla \boldsymbol{N}_p)^T \frac{\boldsymbol{k} k^{rw}}{\mu^w} \nabla \boldsymbol{N}_p\,\mathrm{d}\Omega \\
&\boldsymbol{H}_{gg} = \frac{1}{S_g \rho^g} \int_\Omega (\nabla \boldsymbol{N}_p)^T \frac{\boldsymbol{k} k^{rg}}{\mu^g} \nabla \boldsymbol{N}_p\,\mathrm{d}\Omega \\
&\boldsymbol{H}_{\pi\pi} = \frac{1}{S_\pi \rho^\pi} \int_\Omega (\nabla \boldsymbol{N}_p)^T \frac{\boldsymbol{k} k^{r\pi}}{\mu^\pi} \nabla \boldsymbol{N}_p\,\mathrm{d}\Omega
\end{aligned}
\tag{A.2}
$$

$$
\begin{aligned}
\boldsymbol{f}^u &= \int_\Omega \boldsymbol{N}_u^T((1-n)\rho^s + nS_w\rho^w + nS_g\rho^g + nS_\pi\rho^\pi)\boldsymbol{g}\,\mathrm{d}\Omega + \int_{\Gamma_u^q} \boldsymbol{N}_u^T\bar{\boldsymbol{t}}\,\mathrm{d}\Gamma_u^q \\
\boldsymbol{f}^w &= \frac{1}{S_w\rho^w}\int_\Omega (\nabla \boldsymbol{N}_p)^T \frac{\boldsymbol{k}k^{rw}}{\mu^w}\rho^w\boldsymbol{g}\,\mathrm{d}\Omega - \int_{\Gamma_w^q} \boldsymbol{N}_p^T\frac{\boldsymbol{q}^w}{\rho^w}\,\mathrm{d}\Gamma \\
\boldsymbol{f}^g &= \frac{1}{S_g\rho^g}\int_\Omega (\nabla \boldsymbol{N}_p)^T \frac{\boldsymbol{k}k^{rg}}{\mu^g}\rho^g\boldsymbol{g}\,\mathrm{d}\Omega - \int_{\Gamma_g^q} \boldsymbol{N}_p^T\frac{\boldsymbol{q}^g}{\rho^g}\,\mathrm{d}\Gamma \\
\boldsymbol{f}^\pi &= \frac{1}{S_\pi\rho^\pi}\int_\Omega (\nabla \boldsymbol{N}_p)^T \frac{\boldsymbol{k}k^{r\pi}}{\mu^\pi}\rho^\pi\boldsymbol{g}\,\mathrm{d}\Omega - \int_{\Gamma_\pi^q} \boldsymbol{N}_p^T\frac{\boldsymbol{q}^\pi}{\rho^\pi}\,\mathrm{d}\Gamma
\end{aligned}
\tag{A.3}
$$

where $\boldsymbol{N}_u$ is the vector containing the shape functions for displacement components, $\boldsymbol{N}_p$ is the vector containing the shape functions for pressure of the different phases, $\boldsymbol{B} = \mathbf{L}\boldsymbol{N}_u$ is the matrix relating strain and displacement components, with $\mathbf{L}$ given by Eq. (45).

References

[1] E. Abreu, J. Douglas, F. Furtado, D. Marchesin, F. Pereira Jr., Three-phase immiscible displacement in heterogeneous petroleum reservoirs, Math. Comput. Simulat. 73 (2006) 2–20.
[2] M.A. Biot, P.G. Willis, The elastic coefficients of the theory of consolidation, J. Appl. Mech. 24 (1957) 594–601.
[3] G. Bolzon, B.A. Schrefler, O.C. Zienkiewicz, Elastoplastic soil constitutive laws generalized to partially saturated states, Geotechnique 46 (2) (1996) 279–289.
[4] H.A. Di Rado, P.A. Beneyto, J.L. Mroginski, A.M. Awruch, Influence of the saturation–suction relationship in the formulation of non-saturated soils consolidation models, Math. Comput. Model. 49 (5–6) (2009) 1058–1070.
[5] D.G. Fredlund, H. Rahardjo, Soils Mechanics for Unsaturated Soils, John Wiley & Sons Inc., 1993.
[6] D.G. Fredlund, A. Xing, Equations for the soil–water characteristic curve, Can. Geotech. J. 31 (1994) 521–532.
[7] S.M. Hassanizadeh, W.G. Gray, General conservation equation for multiphase systems: 1. Averaging procedures, Adv. Water Resour. 2 (1979) 131–144.
[8] S.M. Hassanizadeh, W.G. Gray, General conservation equation for multiphase systems: 2. Mass momenta, energy and entropy equations, Adv. Water Resour. 2 (1979) 191–203.
[9] S.M. Hassanizadeh, W.G. Gray, General conservation equation for multiphase systems: 3. Constitutive theory for porous media flow, Adv. Water Resour. 3 (1980) 25–40.
[10] R. Juncosa, J. Samper, N. Vicente, J. Delgado, Formulación numérica en elementos finitos de problemas de flujo multifásico no isotermo y transporte de solutos reactivos en medios porosos, Rev. Int. Métodos Numér. Cálc. Diseño Ing. 18 (3) (2002) 415–432.
[11] N. Khalili, M.H. Khabbaz, On the theory of three-dimensional consolidation in unsaturated soils. in: E.E. Alonso, P. Delage (Eds.), First International Conference on Unsaturated Soils—UNSAT'95, 1995, pp. 745–750.
[12] G. Klubertanz, F. Bouchelaghem, L. Laloui, L. Vulliet, Miscible and immiscible multiphase flow in deformable porous media, Math. Comput. Model. 37 (2003) 571–582.
[13] R.W. Lewis, B.A. Schrefler, Finite element simulation of the subsidence of a gas reservoir undergoing a waterdrive, in: Finite Elements in Fluids, Volume 4 (3rd International Conference on Finite Elements in Flow Problems), John Wiley & Sons, 1982, pp. 179–199.
[14] R.W. Lewis, B.A. Schrefler, N.A. Rahman, A finite element analysis of multiphase immiscible flow in deforming porous media for subsurface systems, Commun. Numer. Meth. Eng. 14 (2) (1998) 135–149.
[15] R.W. Lewis, B.A. Schrefler, The Finite Element Method in the Static and Dynamic Deformation and Consolidation of Porous Media, John Wiley & Sons, 1998.
[16] X. Li, O.C. Zienkiewicz, Multiphase flow in deforming porous media and finite element solutions, Comput. Struct. 45 (2) (1992) 211–227.
[17] B. Loret, N. Khalili, A three-phase model for unsaturated soils, Int. J. Numer. Anal. Meth. 24 (11) (2000) 893–927.
[18] V.D. Murty, C.L. Clay, M.P. Camden, D.B. Paul, Natural convection around a cylinder buried in a porous medium- non-Darcian effects, Appl. Math. Model. 18 (1994) 134–141.
[19] W.K.S. Pao, R.W. Lewis, Three-dimensional finite element simulation of three-phase flow in a deforming fissured reservoir, Comput. Meth. Appl. Mech. 191 (2002) 2631–2659.
[20] B.A. Schrefler, Computer modelling in enviromental geomechanics, Comput. Struct. 79 (2001) 2209–2223.
[21] B.A. Schrefler, F. Pesavento, Multiphase flow in deforming porous material, Comput. Geotech. 31 (2004) 237–250.
[22] D. Sheng, D.W. Smith, Numerical modeling of competitive component with nonlinear adsorption, Int. J. Numer. Anal. Meth. 24 (2000) 47–71.
[23] D. Sheng, D.W. Smith, 2D finite element analysis of multicomponent contaminant transport through soils, Int. J. Geomech. - ASCE. 2 (1) (2002) 113–134.